Electronic Supplementary Material (ESI) for Physical Chemistry Chemical Physics.
This journal is © the Owner Societies 2017

Supporting Information

Molecular Engineering of Lanthanide Ion Chelating Phospholipids Generating Assemblies with a Switched Magnetic Susceptibility

Stéphane Isabettini,*[a] Sarah Massabni,[a] Arnel Hodzic,[a] Dzana Durovic,[a] Joachim Kohlbrecher,[b] Takashi Ishikawa,[c] Peter Fischer,[a] Erich J. Windhab,[a] Peter Walde,[d] and Simon Kuster[a]

[a] Laboratory of Food Process Engineering, ETH Zürich, Schmelzbergstrasse 7, 8092 Zürich, Switzerland.
[b] Laboratory for Neutron Scattering and Imaging, [c] Biomolecular Research Laboratory, Paul Scherrer Institute, 5232 Villigen PSI, Switzerland.
[d] Department of Materials, ETH Zürich, Vladimir-Prelog-Weg 5, 8093 Zürich, Switzerland

E-mail: stephane.isabettini@hest.ethz.ch

Table of Contents

1. Synthesis of DMPE-Glu-DTPA: Description and Characterization

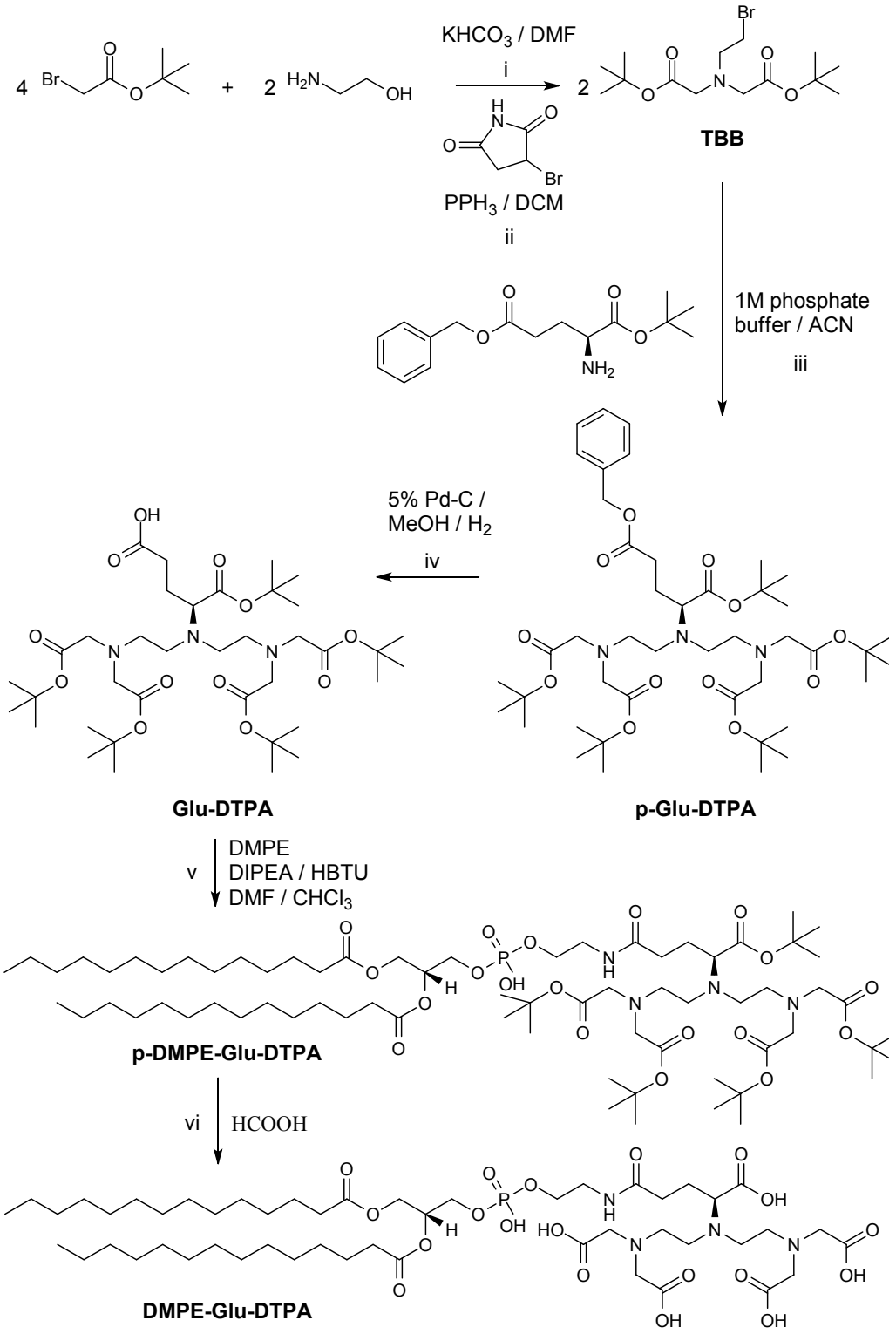

Figure S1. Synthetic pathway for the preparation of DMPE-Glu-DTPA. *i and ii:* synthesis of di-tert-butyl-2-bromoethyliminodiacetate (TBB) as described by Micklitsch *et al*.[1] *iii:* synthesis of p-Glu-DTPA and *iv:* Glu-DTPA inspired from Liebi *et al.*[2] and Anelli *et al*.[3] *v:* Yamada coupling for the synthesis of p-DMPE-Glu-DTPA inspired from Gianella *et al*.[4,5] *vi:* deprotection in formic acid for the synthesis of DMPE-Glu-DTPA as described by M. Liebi et al.[2]

1.1. General Information.

Unless otherwise stated, all chemicals were purchased either from Sigma Aldrich, VWR, Merck or ABCR and employed without further purification. All reactions were conducted according to, or inspired from, published protocols. The reaction scheme along with literature references are presented in Figure S1.

The reactions were conducted in three necked round bottom flasks. They were monitored by analytical thin-layer chromatography (TLC) using silica gel baked on aluminium-foil with a fluorescent indicator 254 nm from RediSep*TM* or Merck. The TLCs were visualized under UV-light at 254 nm. They were further developed by either applying an aqueous alkaline potassium permanganate solution or with a molybdenum phosphorus spray. Solvent evaporation was conducted on a Heidolph Laborota rotary evaporator with a bath temperature of 40 °C and an appropriate pressure. Flash chromatography was performed with a CombyFlash TeledyneIISCO system from Companion using RediSep*TM* Normal phase disposable Columns of various sizes. Separation resolution was improved with 0.1% of 1,1,1,3,3,3-hexafluoro isopropanol purchased from Apollo scientific in the eluent. The yield was calculated based on the mass of the dried and purified compounds.

Nuclear magnetic resonance (NMR) spectra were recorded at room temperature in 5 mm broadband inverse probes on a Bruker spectrometer operating at 400 MHz for ^{1}H-NMR and 100 MHz for ^{13}C-NMR. Unless otherwise stated, deuterated chloroform (ARMAR) was used as a solvent. All NMR spectra were referenced to residual solvent signals. Data is reported as follows: chemical shifts (δ) in parts per million (ppm), if possible identification according to the numeration in the drawn molecular structure, corresponding signal integral, multiplicity abbreviation (s: singlet, d: doublet, t: triplet, q: quartet, m: multiplet). Mass spectra were recorded on an ESI-HRMS from Thermo Scientific (exactive) with direct injection dissolved in an appropriate concentration of methanol. Computed masses were based on single isotope masses for high-resolution spectra. Full calibration was conducted before measurements using the appropriate solutions for both positive and negative modes.

1.2. Synthesis of Di-tert-butyl-2-bromoethyliminodiacetate (TBB)

This synthesis was performed following previously reported protocols.[1,2] Tert-butyl bromoacetate (58.515 g, 300 mmol) and potassium bicarbonate (33.37 g, 333 mmol) were dissolved in 600 ml of anhydrous DMF. The mixture was cooled in an ice bath and ethanolamine (8.14 g, 133 mmol) was added progressively over 10 minutes. The reaction mixture was left to warm up to room temperature and stirred for 24 hours. The reaction volume was reduced to 1/10th of its original volume by removal of DMF under vacuum. 300 ml of a saturated solution of sodium bicarbonate was subsequently added before extracting three times with 400 ml of tert-butyl methyl ether (MTBE). The organic fractions were individually washed twice with a saturated sodium carbonate solution and once with water. The organic fractions were combined, dried over anhydrous sodium sulfate and the solvent removed under vacuum to recover a yellow oil residue. The residue was dissolved in 400 ml of CH_2Cl_2 and triphenylphosphine (38.5 g, 147m mmol) was added at room temperature under stirring. The mixture was cooled down to 5 °C and placed under an Argon atmosphere. N-bromosuccinimide (26.1 g, 147 mmol) was added portion wise over 10 minutes. The reaction mixture was further stirred for 2 hours at 5 °C before the solvent was removed under vacuum. 300 ml of MTBE was added to the resulting oil, causing the formation of a solid. The solid was further extracted with MTBE and the resulting organic phases were combined. After removal of the MTBE under vacuum, the recovered orange oil was purified by flash chromatography using ethyl acetate/heptane (1:9) ramping up from pure heptane. The product was a colorless liquid at room temperature with a **yield** of 72%. **HR-MS(-):** calculated for $C_{14}H_{27}NO_4Br$ [M-H]$^-$: 352.11180. Found: 352.11141. *Δm/z:* 1.1 ppm. **^{1}H-NMR** (400 MHz, $CDCl_3$) δ: 3.47 (s, 4H, -C**H$_2$**-N-C**H$_2$**-), 3.42 (t, 2H, N-CH_2-C**H$_2$**-Br), 3.13 (t, 2H, N-C**H$_2$**-CH_2-Br), 1.44 (s, 18H, BOC) ppm. **^{13}C-NMR** (100 MHz, $CDCl_3$) δ: 170.54, 81.46, 56.59, 30.28, 28.27 ppm.

1.3. Synthesis of p-Glu-DTPA

1 M phosphate buffer (150 ml, pH 8) was added to a solution of H-Glu(OBzl)-O_tBu-HCl (6.611 g, 20 mmol, Christof Senn Laboratories) and tert-butyl N-(2-bromoethyl)iminodiacetate (17.000 g, 48 mmol) in 80 ml of acetonitrile. The reaction mixture was vigorously stirred for 2 hours before the aqueous phase was replaced with 100 ml of fresh buffer. The reaction mixture was further stirred for 48 hours and the organic phase was recovered and dried under vacuum. The residue was dissolved in 150 ml of dichloromethane, washed twice with 20 ml of water, dried over sodium sulfate, and the solvent removed under vacuum. The compound was purified by flash chromatography using ethyl acetate/heptane (1:4) ramping up from pure heptane. The product was a slightly yellow tainted oil with a **yield** of 55%. **HR-MS(+):** calculated for $C_{44}H_{74}N_3O_{12}$ $[M+H]^+$: 836.5267. Found: 836.5269. *Δm/z:* 0.2 ppm and for $C_{44}H_{73}N_3O_{12}Na$ $[M+Na]^+$: 858.5087. Found: 858.5082. *Δm/z:* 0.6 ppm. **^{1}H-NMR** (400 MHz, $CDCl_3$) δ: 7.28 – 7.38 (m, 5H, Ph), 5.10 (s, 2H, Ph-C**H_2**-O-), 3.41 (s, 8H, -N-C**H_2**-CO-), 3.34 (m, 1H, -CO-CH_2-CH_2-C**H**-), 2.67-2.79 (m, 8H, -N-C**H_2**-C**H_2**-N-), 2.38-2.55 (m, 2H, -CO-C**H_2**-CH_2-CH-), 1.79-2.05 (m + m, 1H + 1H, -CO-CH_2-C**H_2**-CH-), 1.44-1.45 (s + s, 45H, BOC) ppm. **^{13}C-NMR** (100 MHz, $CDCl_3$) δ: 171.88, 170.36, 170.26, 135.99, 128.31, 128.16, 127.99, 127.91, 80.68, 80.55, 80.43, 65.85, 63.16, 55.82, 53.61, 50.01, 30.68, 28.11, 28.06, 27.98, 24.73.

1.4 Synthesis of Glu-DTPA

0.104 g of Palladium (5%) on activated carbon were added to a 20 ml methanol solution containing p-Glu-DTPA (1.778 g, 2.2 mmol). 1 ml of acetic acid and 1 ml of water were added and the suspension was stirred for 2 hours under a hydrogen atmosphere at 20 °C. The reaction was monitored by TLC with ethanol/chloroform (1:15) where the product had an R_f of 0.3 and the reactant had an R_f of 0.8. The reaction mixture was filtered through Celite Hyflo Supercell (0.45 µm). The filter waters were further purified by flash chromatography using isocratic ethanol/chloroform (1:15). The product was a colorless oil with a **yield** of 98%. **HR-MS(+):** calculated for $C_{37}H_{68}N_3O_{12}$ $[M+H]^+$: 746.4798. Found: 746.4804. *Δm/z:* 0.8 ppm and for $C_{37}H_{67}N_3O_{12}Na$ $[M+Na]^+$: 768.4617. Found: 768.4617. *Δm/z:* 0.0 ppm. **^{1}H-NMR** (400 MHz, $CDCl_3$) δ: 3.55 (m, 1H, -CO-CH_2-CH_2-C**H**-), 3.34 (s, 8H, -N-C**H_2**-CO-), 2.67-2.81 (m, 8H, -N-C**H_2**- C**H_2**-N-), 2.37-2.54 (m, 2H, -CO-C**H_2**-CH_2-CH-), 1.74-1.97 (m + m, 1H + 1H, -CO-CH_2-C**H_2**-CH-), 1.37-1.38 (s + s, 45H, BOC) ppm. **^{13}C-NMR** (100 MHz, $CDCl_3$) δ: 177.14, 170.44, 81.36, 80.97, 63.76, 55.73, 53.18, 49.85, 32.01, 28.23, 28.13, 24.48 ppm.

1.5 Synthesis of p-DMPE-Glu-DTPA

A Yamada reaction was employed to couple the Glu-DTPA to DMPE with an amide bond.[4,5] Glu-DTPA (4.26 g, 5.7 mmol) was dried three times by a toluene distillation and dissolved in 40 ml of anhydrous DMF. N,N-Diisopropylethylamine (2.96 g, 22.8 mmol) and HBTU (2.014 g, 5.3 mmol) were subsequently added. The reaction mixture was stirred for 30 minutes and monitored by TLC with ethanol/chloroform (1:10). 60 ml of anhydrous chloroform containing DMPE (3.56 g, 5.6 mmol, COATSOME) was added to the reaction mixture, which was placed under nitrogen atmosphere and further stirred for 5 hours at room temperature. The reaction was monitored by TLC with ethanol/chloroform (1:7). Unreacted solids were filtered out of the reaction mixture before adding 500 ml of chloroform. The mixture was washed twice with 150 ml of 0.5 M citric acid, once with 200 ml of saturated sodium chloride solution, and once with 200 ml of water. The organic fraction was dried over anhydrous sodium sulfate and the solvents removed under vacuum. The oily residue was purified by flash chromatography using isocratic ethanol/chloroform (1:7). The product was a slightly yellow oil with a **yield** of 41 %. **HR-MS(-):** calculated for $C_{70}H_{130}N_4O_{19}P$ $[M-H]^-$: 1361.90724. Found: 1361.9066. *Δm/z:* 0.5 ppm. **^{1}H-NMR** (400 MHz, CDCl3) δ: 5.13 (m, 1H, DMPE), 4.35-4.32 (m, 1H, DMPE), 4.11-4.06 (m, 1H, DMPE), 3.90 (m, 4H, DMPE), 3.64-3.59 (q, 1H, Glu-DTPA), 3.55-2.40 (m, 24H, DMPE and Glu-DTPA), 2.30 (m, 2H, Glu-DTPA), 2.23-2.18 (m, 4H, DMPE), 1.94 (m, 2H, Glu-DTPA), 1.52 (m, 4H, DMPE), 1.40 (s, 45H, BOC from Glu-DTPA), 1.19 (m, 40H, DMPE), 0.82 (t, 6H, terminal CH_3 from myristoyl tails of DMPE) ppm. **^{13}C-NMR** (100 MHz, $CDCl_3$) δ: 173.02, 172.89, 171.13, 81.89, 70.57, 70.49, 63.81, 63.47, 62.75, 57.95, 56.06, 52.26, 48.94, 41.06, 34.30, 34.12, 31.93, 29.71, 29.56, 29.37, 29.18, 28.17, 28.15, 24.94, 24.90, 22.69, 18.43, 14.11 ppm.

1.6 Synthesis of DMPE-Glu-DTPA

1 g of p-DMPE-Glu-DTPA from was dried with three toluene distillations before 20 ml of formic acid was added and the mixture heated to 50 °C. The reaction was placed under nitrogen atmosphere and stirred for 24 hours. The reaction mixture became cloudy and could be monitored by TLC with ammonium hydroxide/ethanol/chloroform (2:5:5). The formic acid was removed under vacuum and the residue dissolved in a mixture of methanol/chloroform (1:4) and crystalized by the addition of acetonitrile. The recovered yellow powder was purified by flash chromatography starting with isocratic methanol/chloroform (1:4) for 3 column volumes. The solvent system was then switched to ammonium hydroxide/ethanol/chloroform (2:5:5) to recover the product as a white powder. The product was re-crystalized with methanol/chloroform (1:4) and acetonitrile for additional purity. The product was stored under Argon in the freezer and a **yield** of 30 % was obtained. **HR-MS(+):** calculated for $C_{50}H_{92}N_4O_{19}P$ $[M+H]^+$: 1083.60879. Found: 1083.6082. *Δm/z:* 0.5 ppm and for $C_{50}H_{91}N_4O_{19}PNa$ $[M+Na]^+$: 1105.59073. Found: 1105.5895. *Δm/z:* 1.1 ppm. **HR-MS(-):** calculated for $C_{50}H_{90}N_4O_{19}P$ $[M-H]^-$: 1081.59424. Found: 1081.5947. *Δm/z:* 0.4 ppm. DMPE-Glu-DTPA was not soluble in chloroform and had to be dissolved in CMW (deuterated solvent mixture composed of $CDCl_3$, CD_3OD and D_2O in a ratio of 80:20:1) in an acidic environment provided by a drop of DCl for ^1H and ^{13}C-NMR. The likely existence of polymolecular assemblies during measurement and the presence of five carboxylic acids considerably reduces the resolution of the spectra. Nevertheless, the obtained spectra confirm the successful synthesis of the compound by the characteristic phospholipid and headgroup peaks. The mixture was calibrated on the chloroform residual solvent signal at 7.26 ppm for ^1H-NMR and 77.16 ppm for ^{13}C-NMR. **^{1}H-NMR** (400 MHz, CMW + a drop of DCl) δ: 5.45 (m, 10H, DMPE and Glu-DTPA), 5.18 (m, 1H, DMPE), 3.0-4.5 (m, 21H, DMPE and Glu-DTPA), 2.55 (m, 2H, Glu-DTPA), 2.26 (m, 4H, DMPE), 2.11 (m, 2H, Glu-DTPA), 1.54 (m, 4H, DMPE), 1.22 (m, 40H, DMPE), 0.81 (t, 6H, terminal CH_3 from myristoyl tails of DMPE) ppm. **^{13}C-NMR** (100 MHz, CMW+ a drop of DCl) δ: 174.83, 173.89, 173.49, 167.75, 69.75, 65.69, 65.07, 62.26, 55.42, 53.44, 46.97, 39.95, 37.46, 34.18, 34.07, 32.77, 31.91, 29.68, 29.57, 29.35, 29.15, 27.10, 24.87, 22.66, 19.72, 14.05 ppm.

2. Mass Spectra of the Synthesized Compounds

p-Glu-DTPA

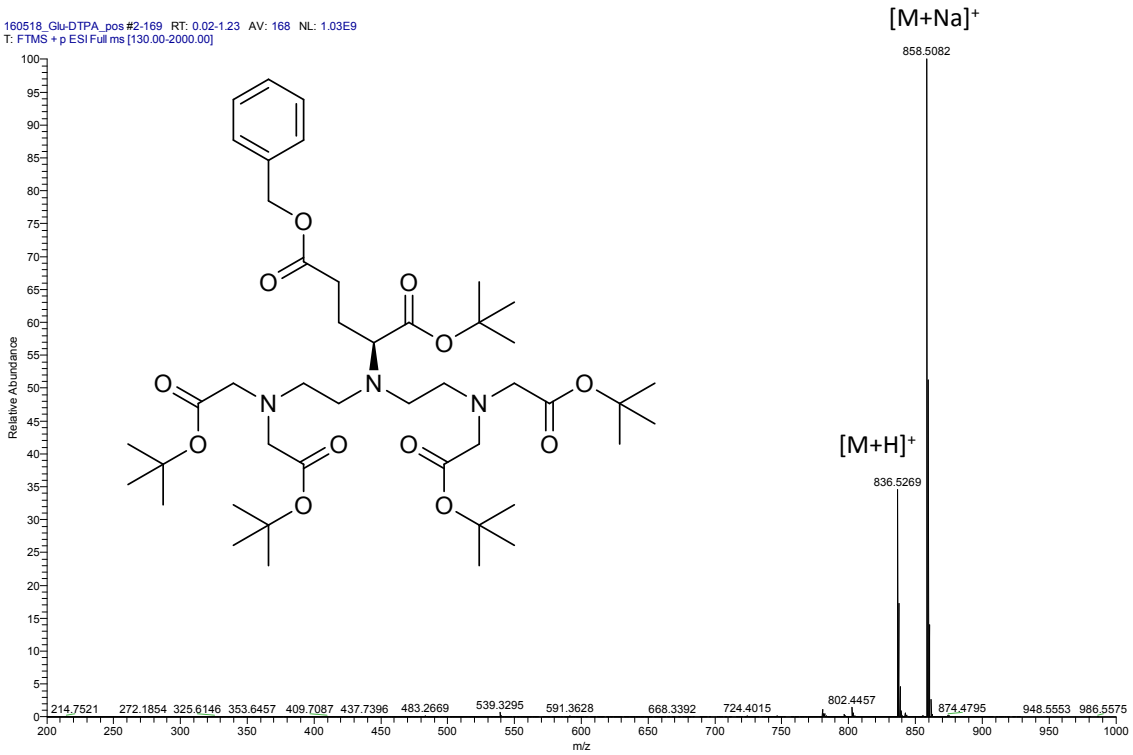

Glu-DTPA

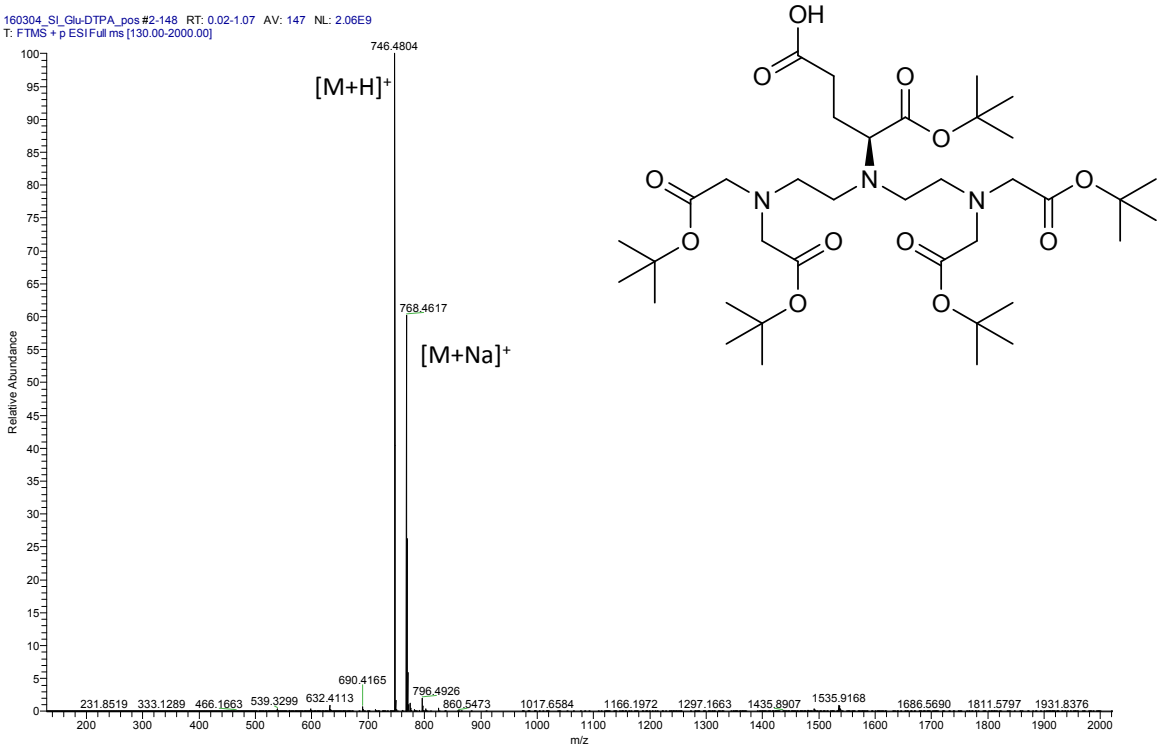

p-DMPE-Glu-DTPA

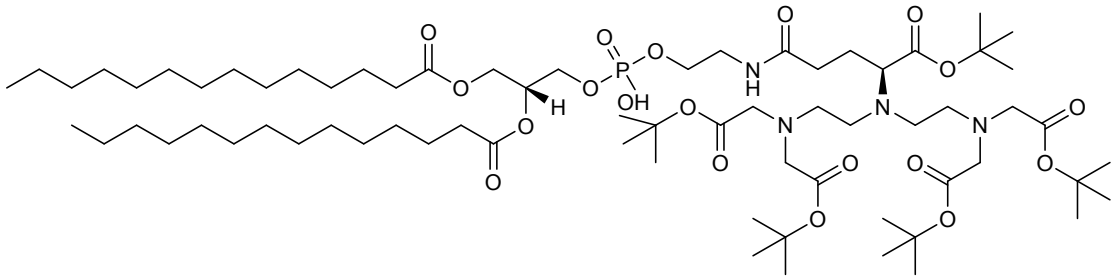

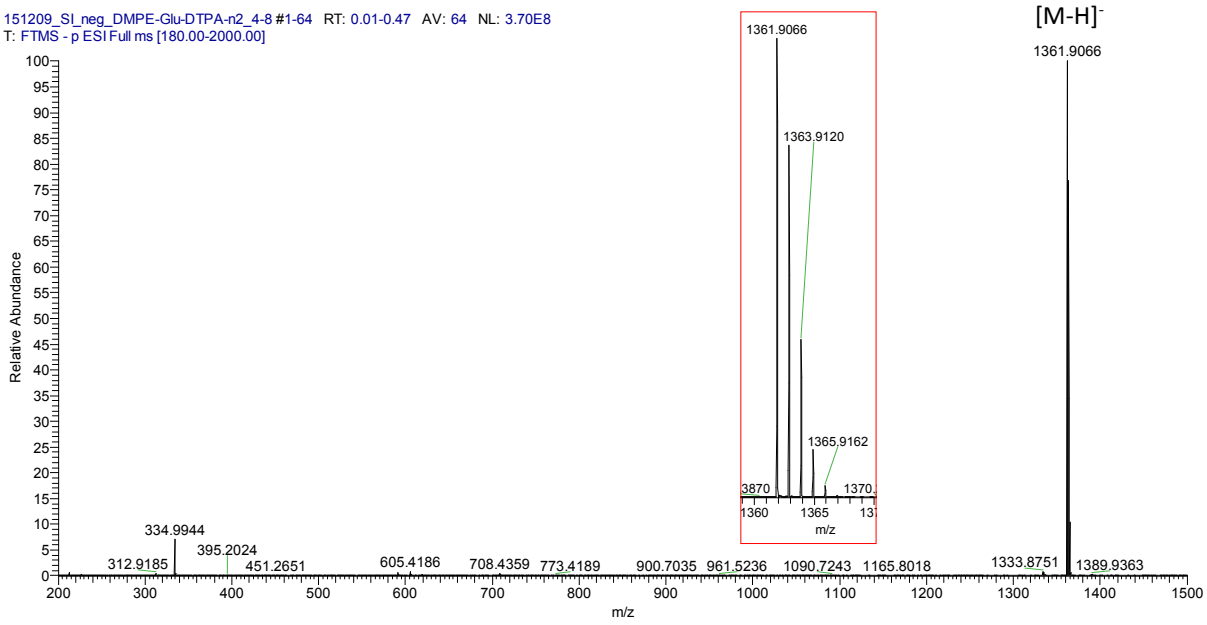

DMPE-Glu-DTPA

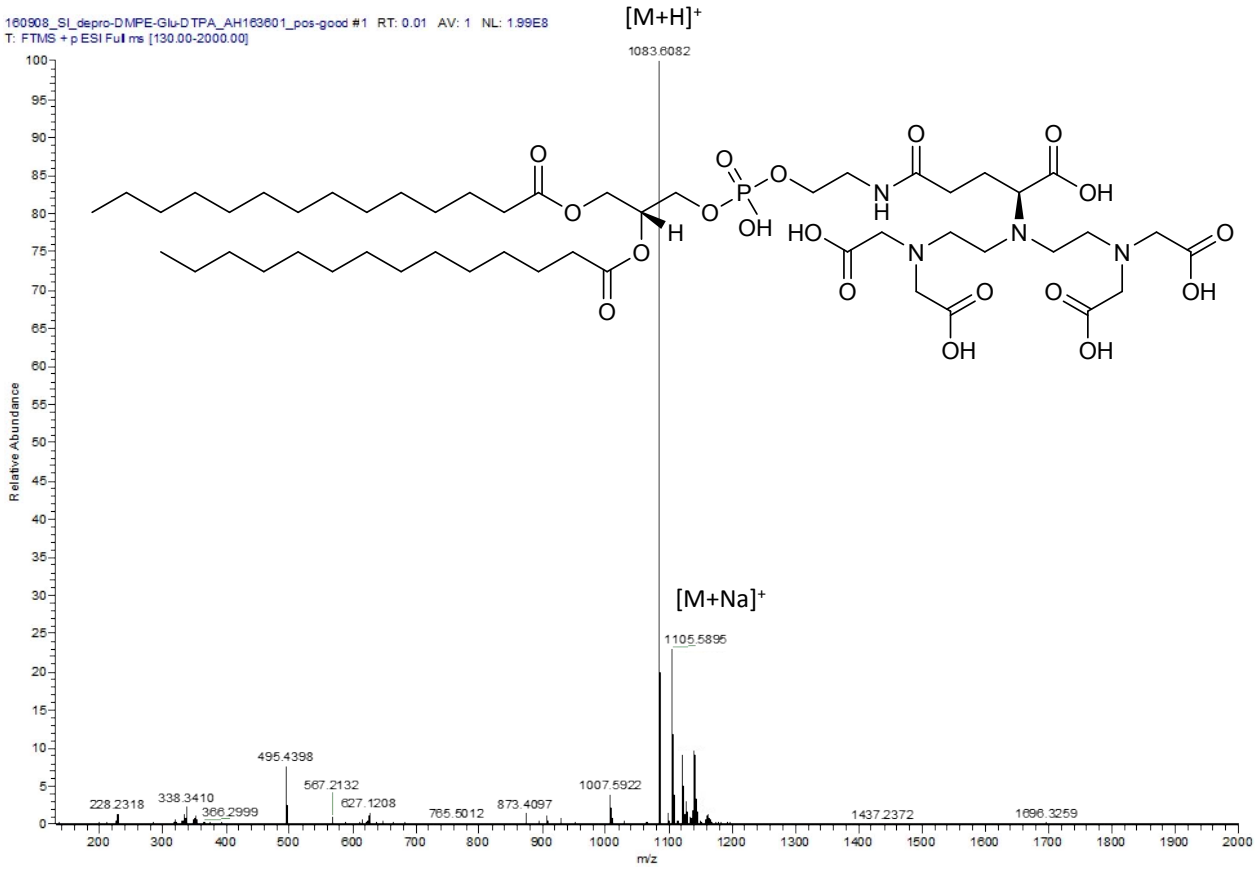

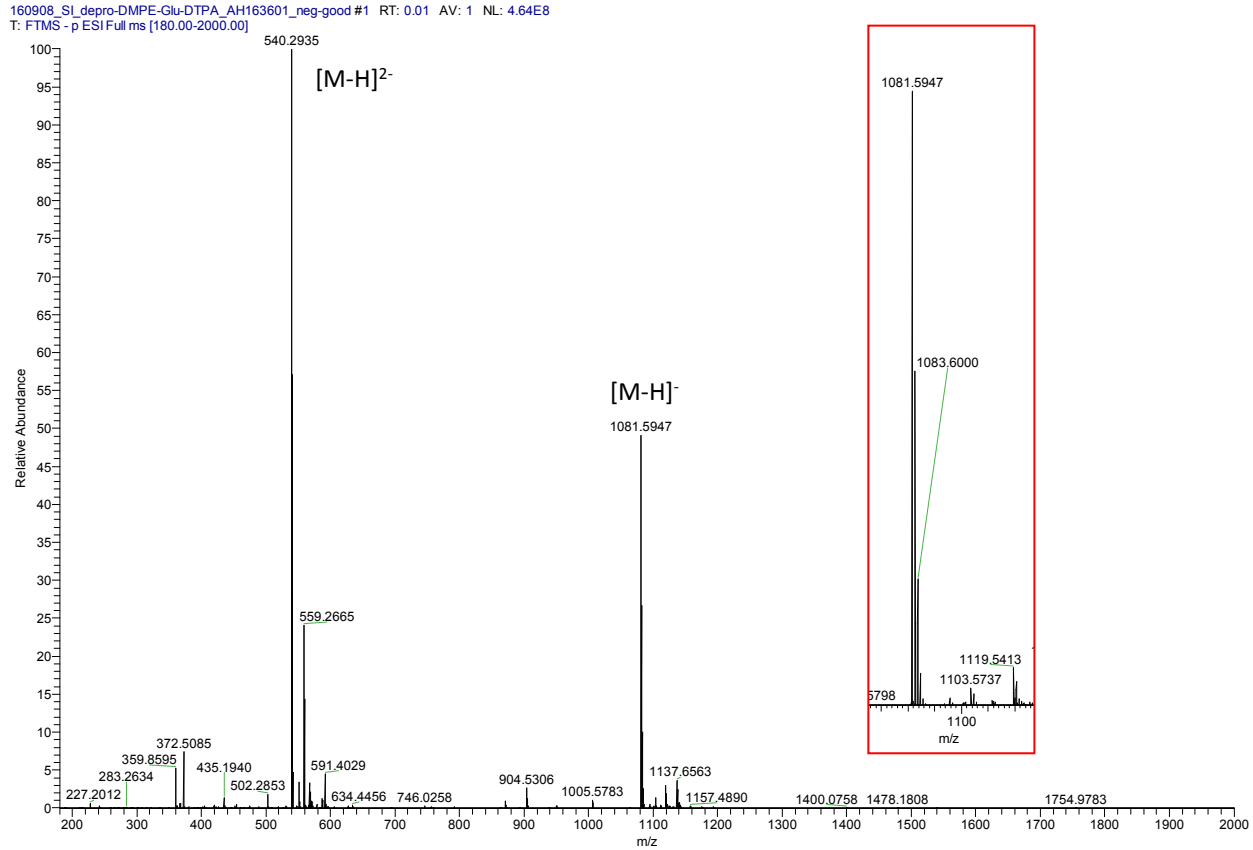

3. ^{1}H-NMR Spectra of the Synthesized Compounds

Di-tert-butyl-2-bromoethyliminodiacetate (TBB)

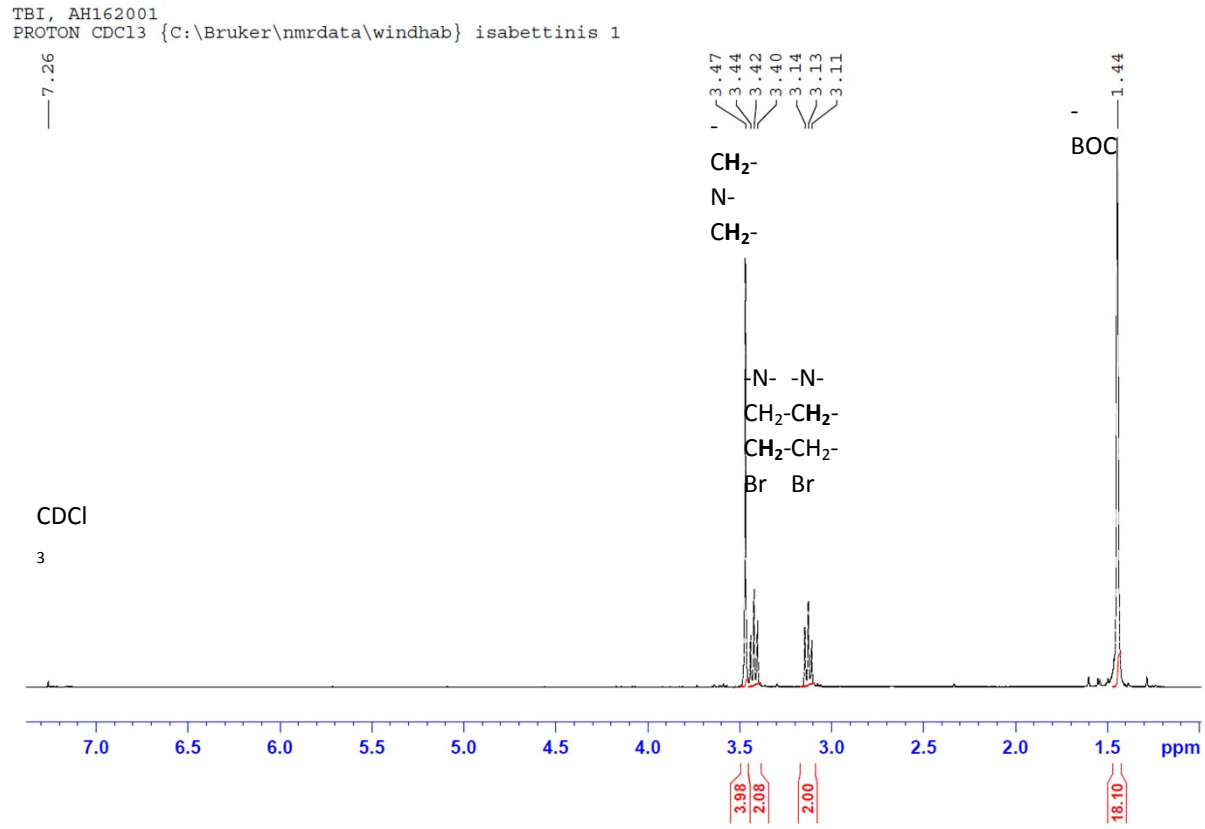

p-Glu-DTPA

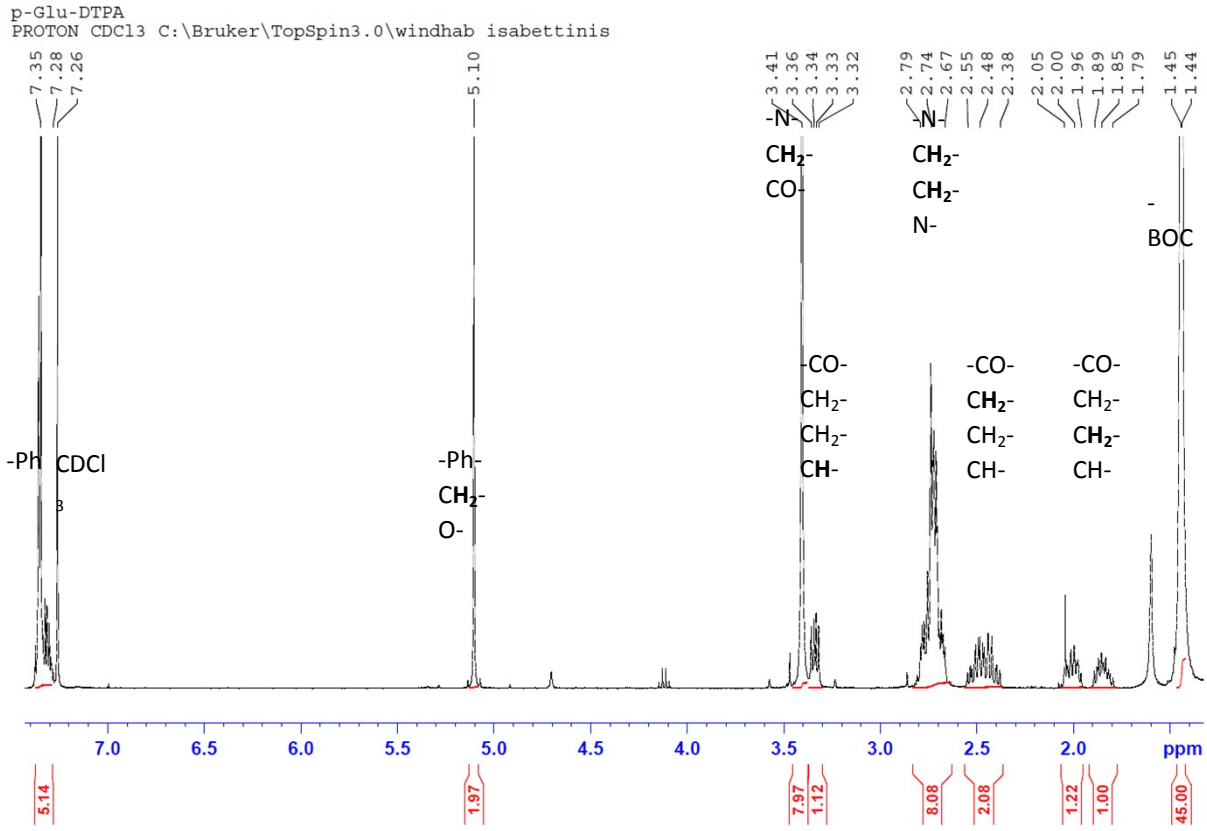

Glu-DTPA

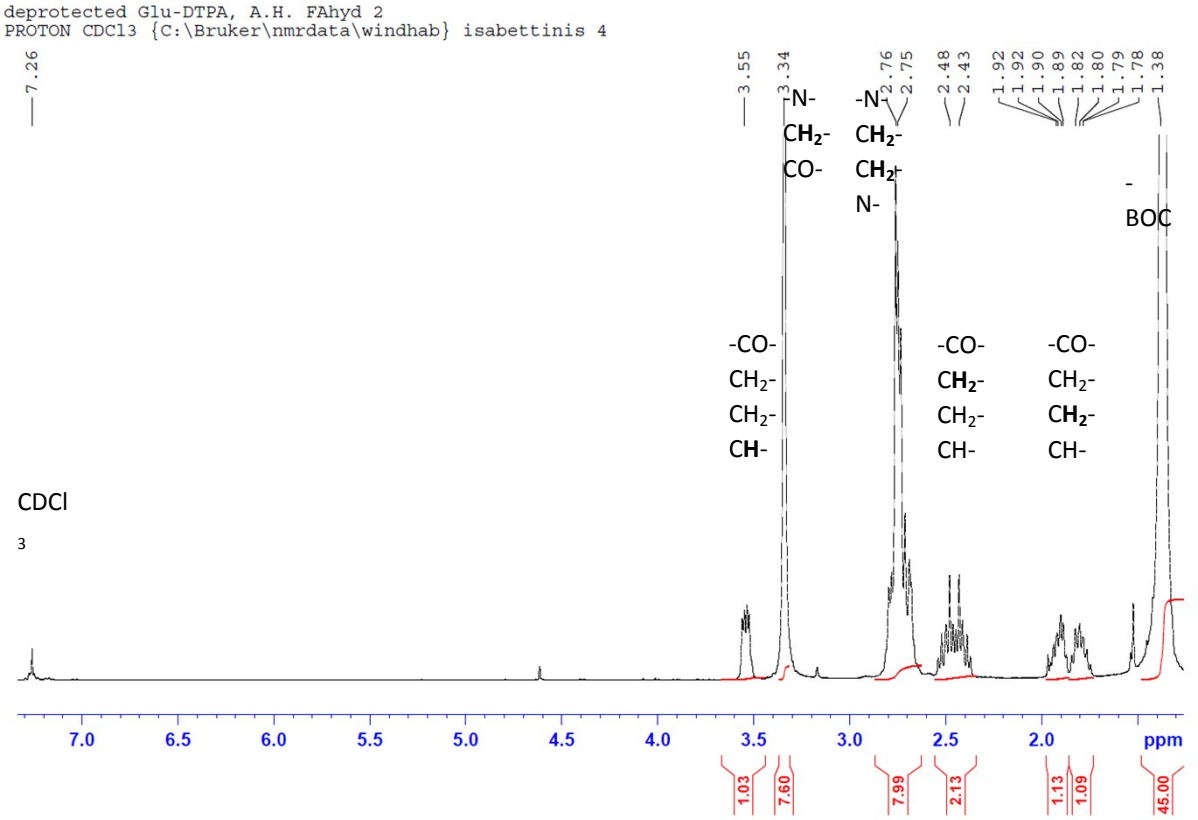

p-DMPE-Glu-DTPA

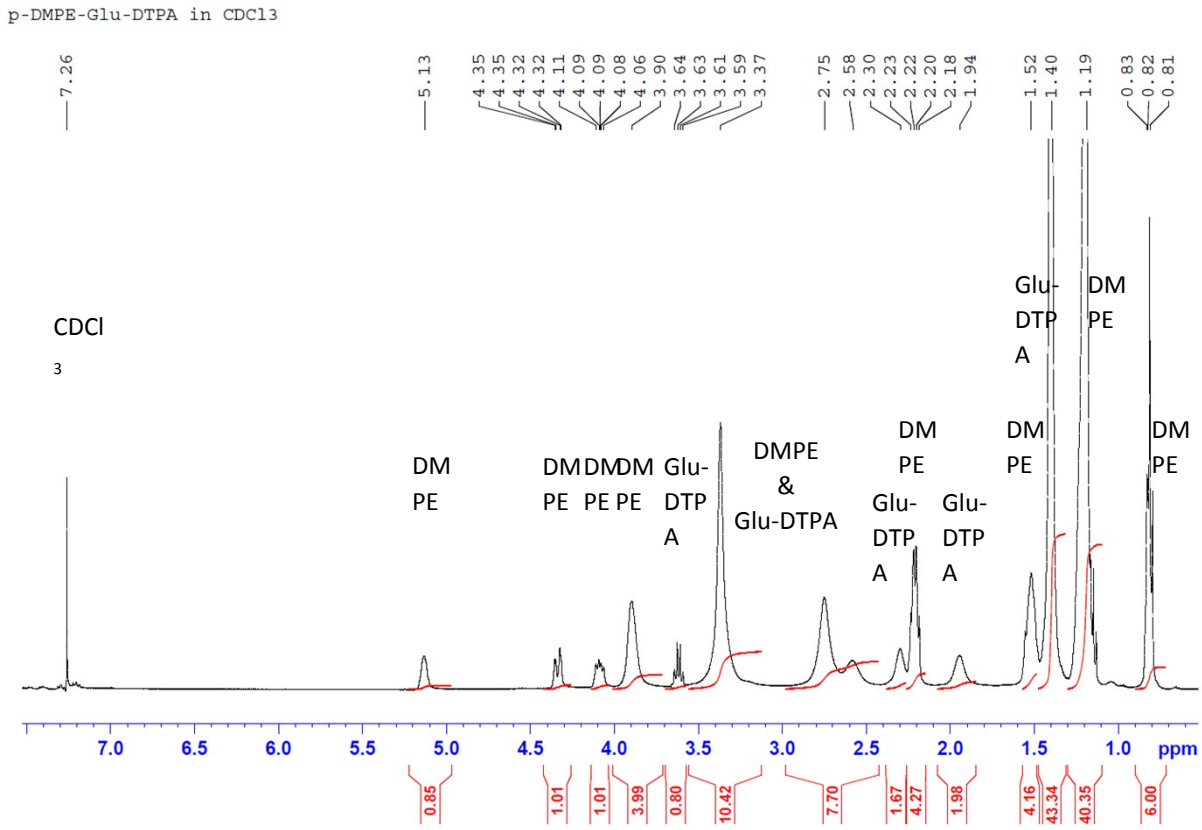

DMPE-Glu-DTPA

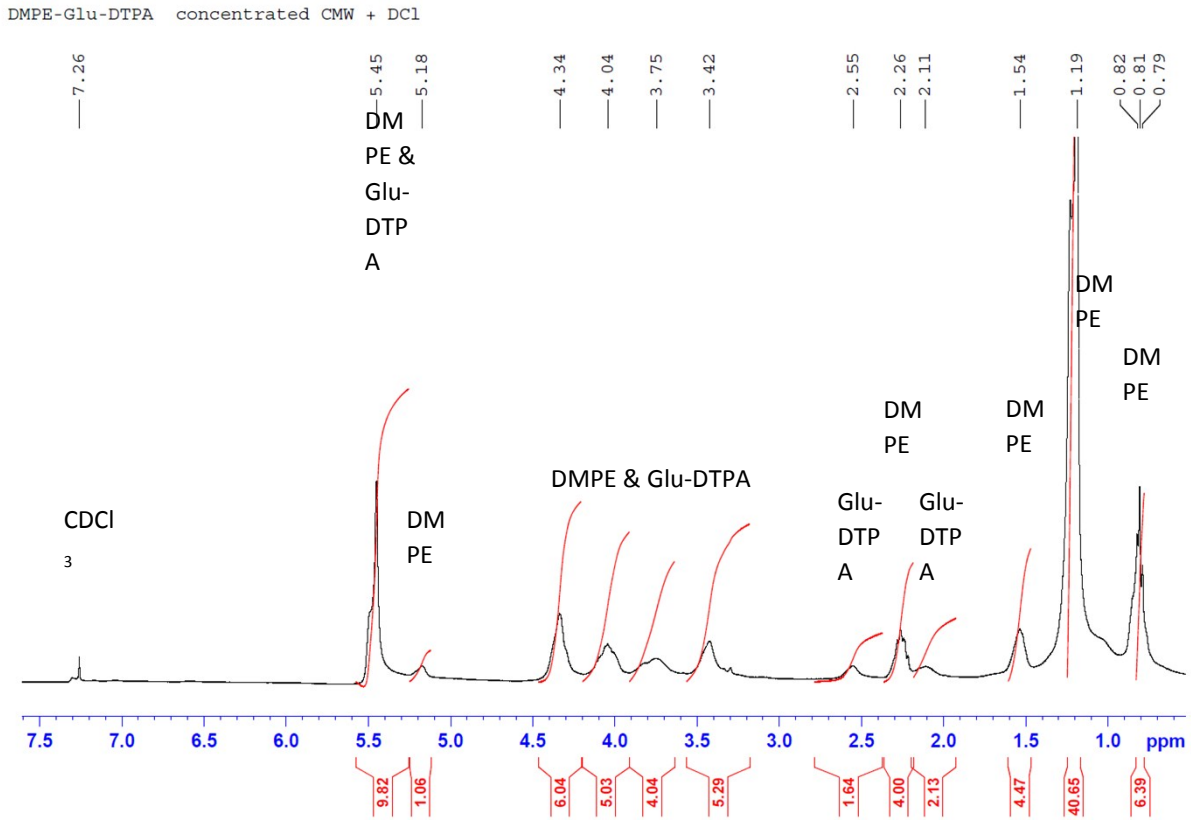

4. ^{13}C-NMR Spectra of the Synthesized Compounds

Di-tert-butyl-2-bromoethyliminodiacetate (TBB)

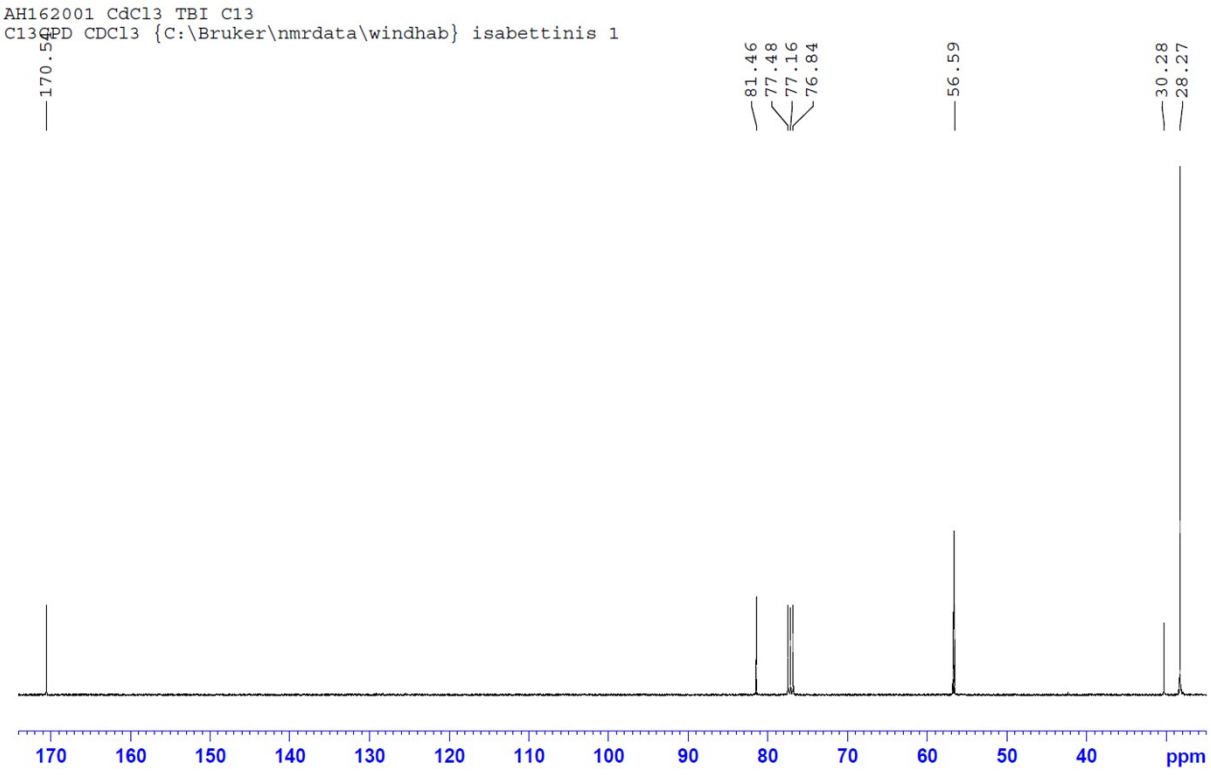

p-Glu-DTPA

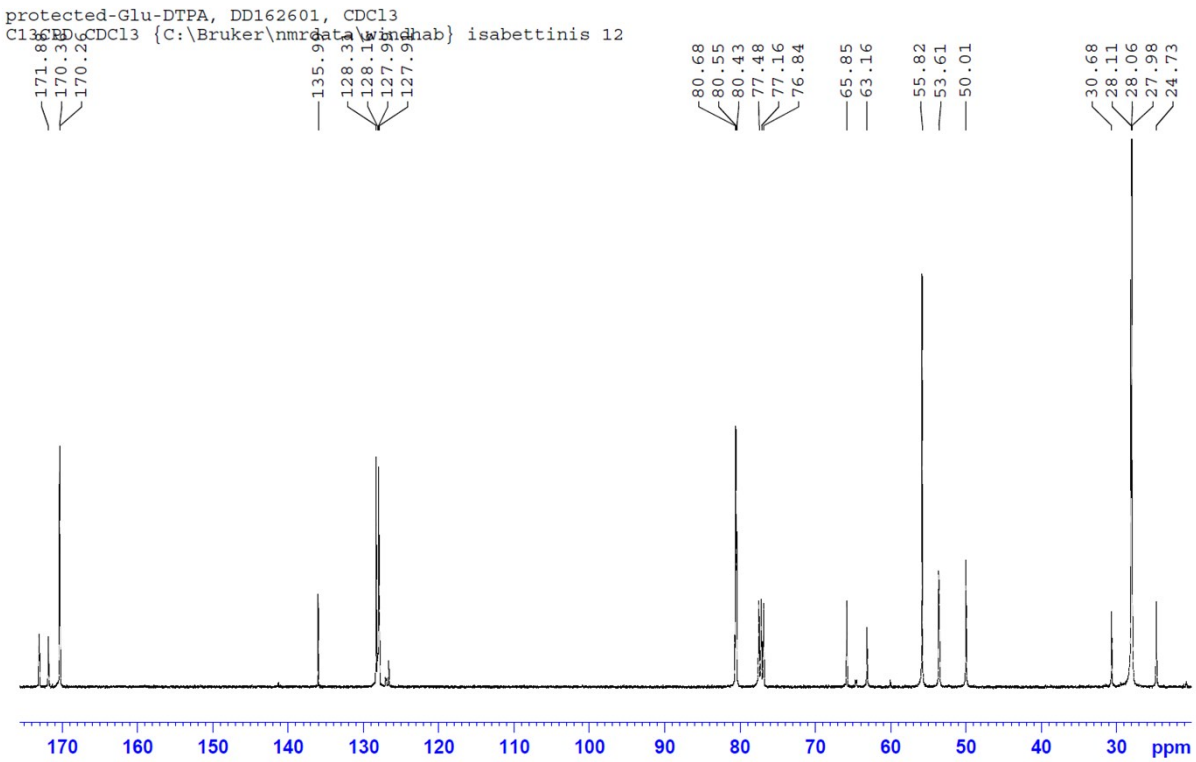

Glu-DTPA

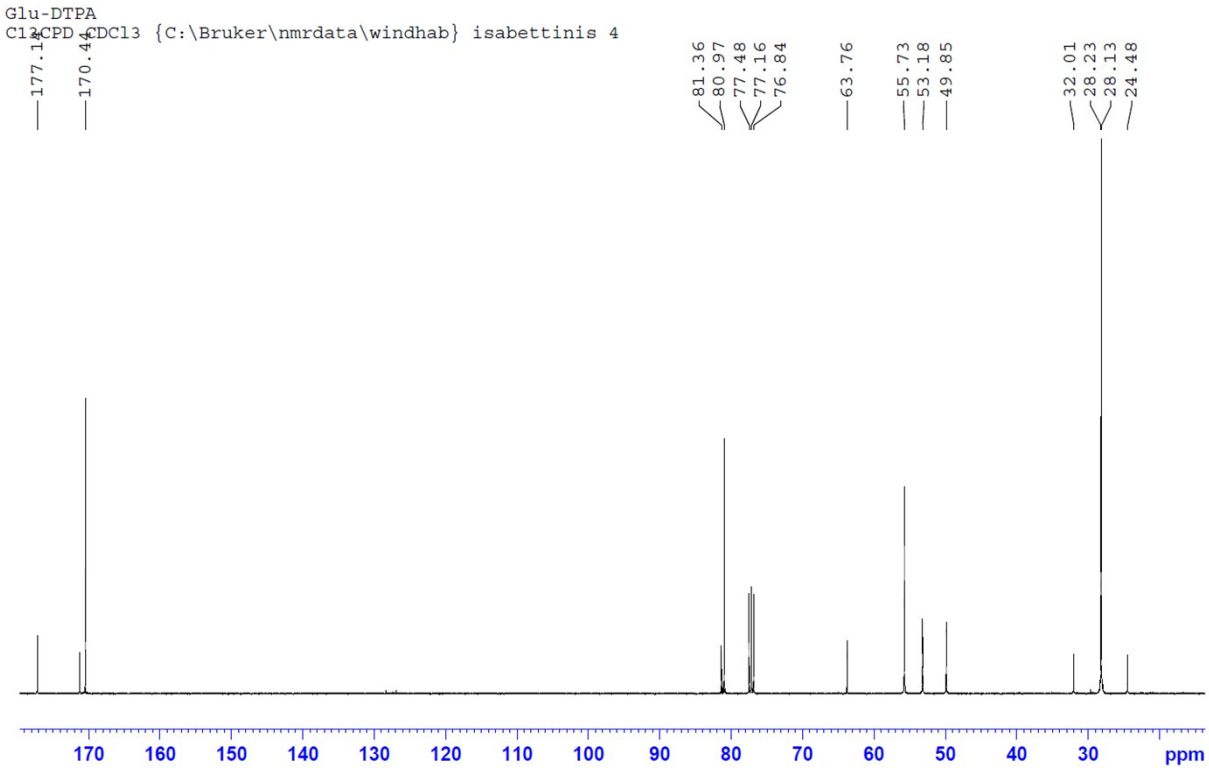

p-DMPE-Glu-DTPA – Full Spectra

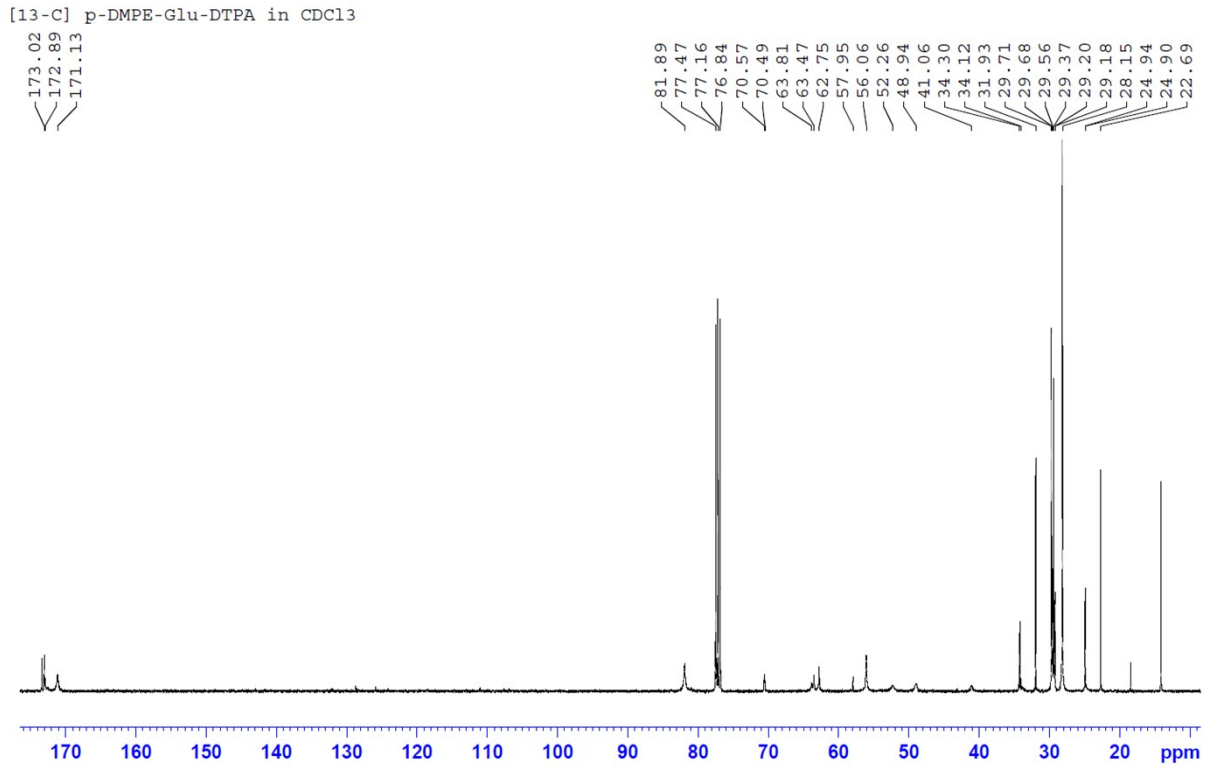

p-DMPE-Glu-DTPA – Zoom In (12 - 85 ppm)

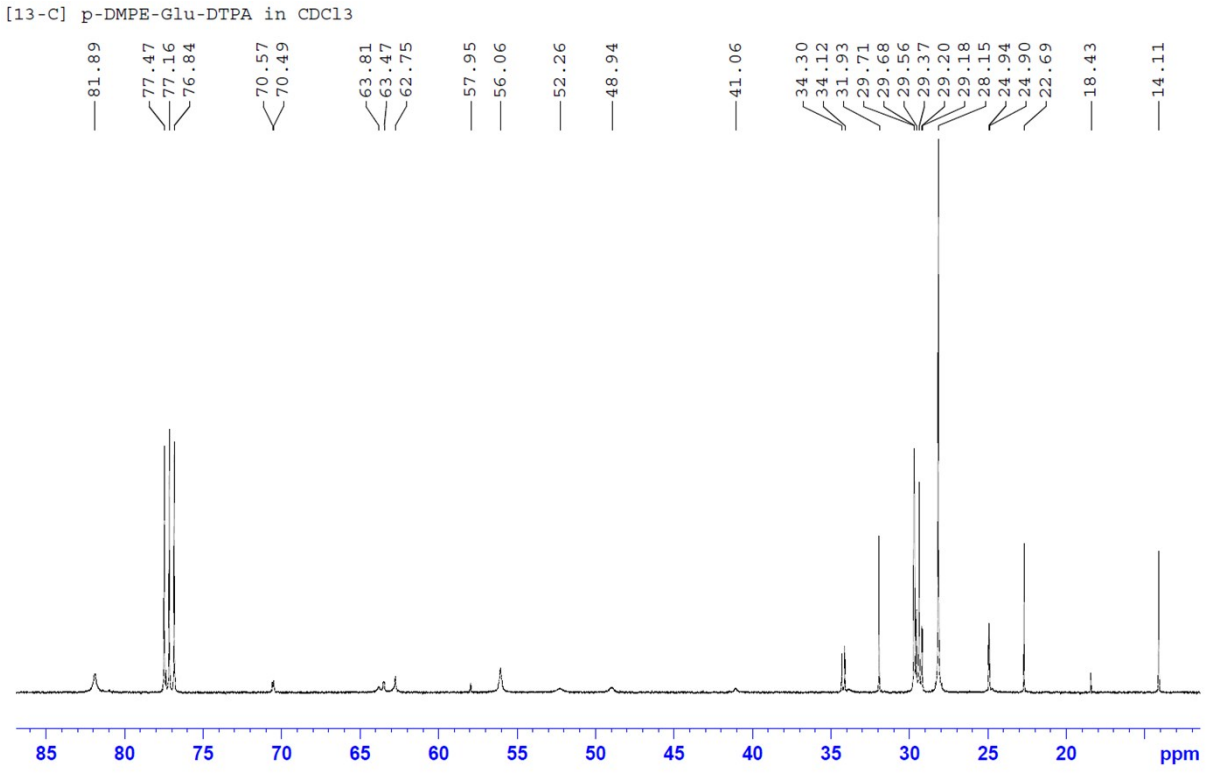

DMPE-Glu-DTPA – Full Spectra

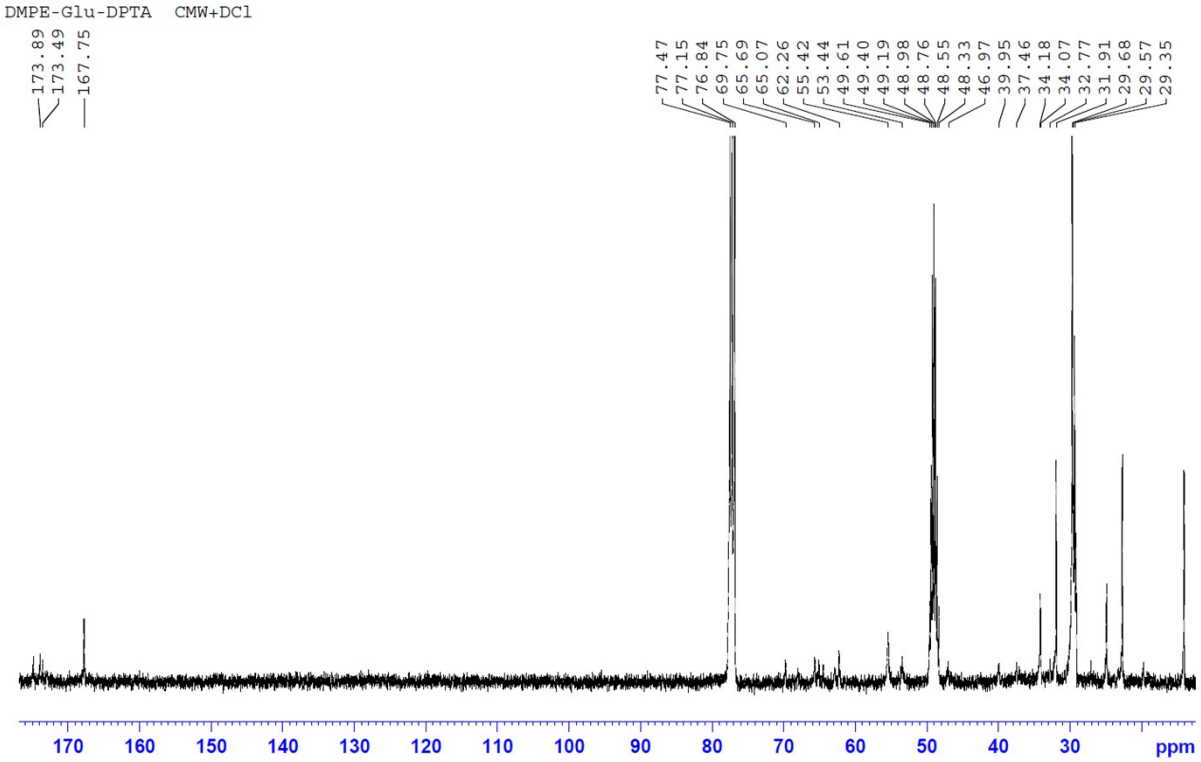

DMPE-Glu-DTPA – Zoom In (12 - 80 ppm)

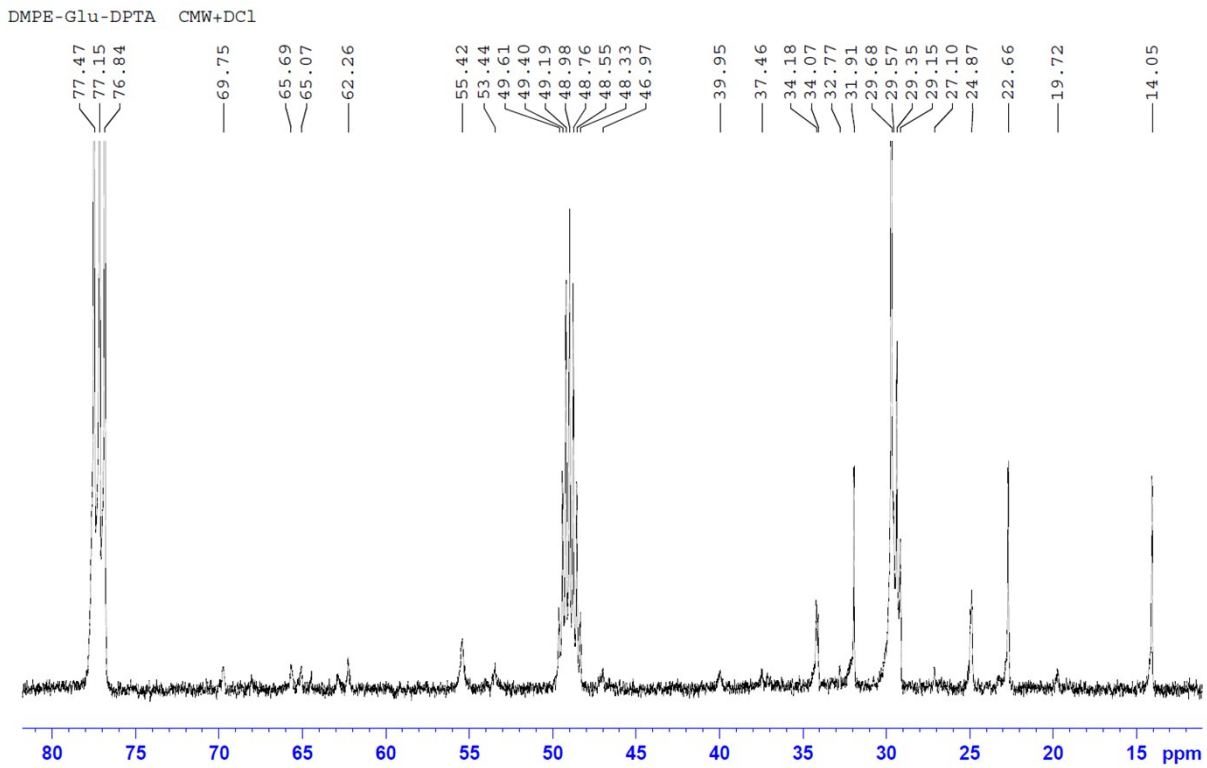

2. Impact of changing the molar ratio of DMPC/DMPE-Glu-DTPA/Tm^{3+} on the magnetic response and structure of the polymolecular assemblies

The dimensions and magnetic response of the DMPC/DMPE-Glu-DTPA/Ln^{3+} assemblies were optimized by altering the lipid molar ratio of the constituting lipids. This technique is commonly employed to tailor the magnetic alignment in DMPC/DHPC bicelles through their size.[6] The lipid molar ratio is also crucial in DMPC/DMPE-DTPA/Ln^{3+} systems to generate highly magnetically alignable bicelles.[7,8] Therefore, the magnetic alignment achieved at different molar ratios of DMPC/DMPE-Glu-DTPA/Tm^{3+} of 7:1:1, 5:1:1, 3:1:1, and 3:2:2 was monitored by the birefringence signal and compared to the 4:1:1 system as a reference, see Figure S2.

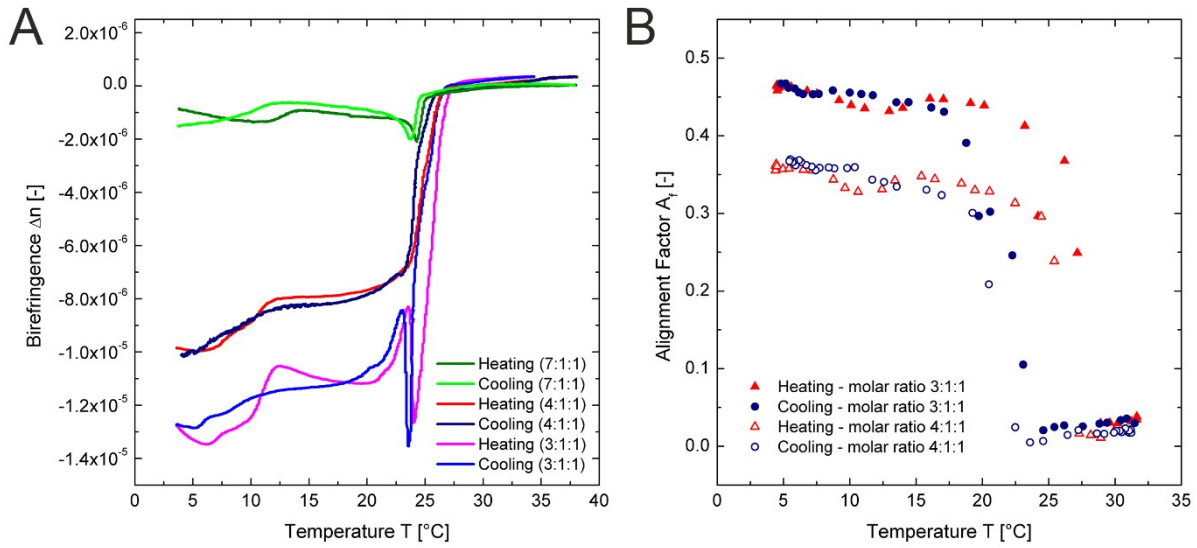

Figure S2. A) Evolution of the birefringence signal under a 5.5 T magnetic field as a function of temperature. DMPC/DMPE-Glu-DTPA/Tm^{3+} (molar ratio 4:1:1) was compared to different molar ratios of 7:1:1 and 3:1:1. The total lipid concentration was 15 mM in a 50 mM phosphate buffer at a pH value of 7.4. B) Evolution of the alignment factor A_f of DMPC/DMPE-Glu-DTPA/Tm^{3+} molar ratio 4:1:1 and 3:1:1 under a 8 T magnetic field as a function of temperature. All heating and cooling was conducted at 1 °C/min.

DMPC/DMPE-Glu-DTPA/Tm^{3+} (molar ratio 3:2:2) showed no signs of alignment. The cone-like nature of the DMPE-Glu-DTPA/Tm^{3+} complex may have induced too much curvature in the bilayer at such a high lipid content. The resulting possible formation of small bicelles or even micellar assemblies could explain the absence of a magnetic response. All the other investigated samples switched the alignment direction when exposed to an external magnetic field. These findings confirm the capacity of the engineered Ln^{3+} chelating DMPE-Glu-DTPA phospholipid to provide a dramatically different magnetic susceptibility $\Delta\chi$. Both DMPC/DMPE-Glu-DTPA/Tm^{3+} samples with a molar ratio of 7:1:1 and 5:1:1 revealed similar weak birefringence signals. However, the signal followed an analogous trend to that of the reference DMPC/DMPE-Glu-DTPA/Tm^{3+} (molar ratio 4:1:1) system with changing temperature, see Figure S2A. A characteristic thermoreversible collapse of the birefringence signal occurred above the phase transition temperature T_m of DMPC at 24 °C. Therefore, the weak birefringence signal probably originated from the alignment of similar assembly structures in the magnetic field. However, the lipid content remained too low to effectively form highly alignable species. DMPC/DMPE-Glu-DTPA/Tm^{3+} (molar ratio 3:1:1) delivered a stronger birefringence signal than the reference system, see Figure S2. The higher magnetic alignability was confirmed by SANS measurements at 5 °C and 8 T, revealing an alignment factor A_f of 0.47, up from 0.36 obtained with the reference DMPC/DMPE-Glu-DTPA/Tm^{3+} (molar ratio 4:1:1) system. Analogously to the birefringence results, larger alignment factors A_f were obtained over the studied temperature range on heating and cooling, see Figure S2B. The structure of these polymolecular assemblies was further studied by cryo-TEM and SANS to identify the origins of the enhanced magnetic response.

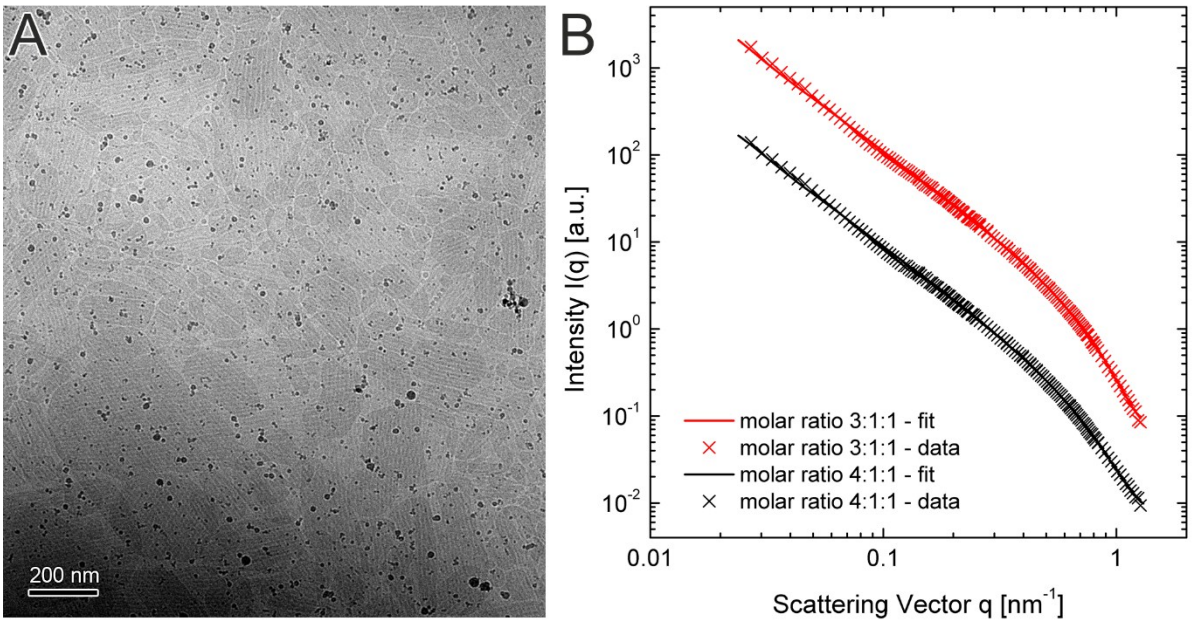

Figure S3. A) Cryo-TEM micrographs of DMPC/DMPE-Glu-DTPA/Tm^{3+} (molar ratio 3:1:1) flash-frozen at 5 °C. Ripples appear as regular darker lines on the planar surface of the assemblies. The scale bar represents 200 nm. High contrast particles are ice crystals resulting from the freezing procedure. B) Radially averaged SANS curves (data points) and corresponding fits (filled lines) at 5 °C of DMPC/DMPE-Glu-DTPA/Tm^{3+} molar ratio 4:1:1 (black) and 3:1:1 (red). All samples were fitted with a form factor for Porod cylinders with a lognormal distribution. The disk thickness was 4.2 nm with an average radius and standard deviation of 94 nm and σ 0.23 for the molar ratio 4:1:1 and 105 nm and σ 0.22 for the molar ratio 3:1:1. The curves were shifted vertically for clarity.

The cryo-TEM micrograph of DMPC/DMPE-Glu-DTPA/Tm^{3+} (molar ratio 3:1:1) flash frozen at 5 °C in Figure S3A revealed similar asymmetric polymolecular assemblies with ripples as those observed in the reference DMPC/DMPE-Glu-DTPA/Tm^{3+} (molar ratio 4:1:1) in Figure 3. The assemblies were polydisperse in size and the higher magnetic alignment could originate from larger species. These findings were confirmed from the radially averaged SANS curve of the sample at 5 °C in the absence of a magnetic field in Figure S3B. The data was fitted with a form factor for Porod cylinders and a lognormal distribution. The bilayer thickness was 4.2 nm, the radius 105 nm, and the standard deviation $\sigma = 0.22$. These findings confirm that the DMPC/DMPE-Glu-DTPA/Tm^{3+} (molar ratio 3:1:1) assemblies were on average larger than the reference DMPC/DMPE-Glu-DTPA/Tm^{3+} (molar ratio 4:1:1) species. Therefore, the enhanced magnetic response of the former originates from their larger size, having more bilayer lipids contributing to the overall magnetic energy of the polymolecular assembly.

3. The importance of the phosphate buffer for generating optimally magnetically responsive DMPC/DMPE-Glu-DTPA/Tm^{3+} assemblies.

Working with a 50 mM phosphate buffer at a pH value of 7.4 is essential to guaranty the optimal formation of DMPC/DMPE-DTPA/Ln^{3+} bicellar systems. Controlling the pH is necessary to compensate the acidic nature of the lanthanide salts and enable optimal chelation of the Ln^{3+}.[7,8] The phosphate buffer dictates the electrostatic forces surrounding the polymolecular assemblies, influencing their architecture. Many structural phenomena observed on assemblies made from a phospholipid bilayer are induced by the buffer. This is particularly true for the appearance of ripples.[9] Herein, we investigate the polymolecular assemblies resulting from DMPC/DMPE-Glu-DTPA/Tm^{3+} (molar ratio 4:1:1) in water and their magnetic alignability. The pH was adjusted to a value of 7.4 by titration with 1M NaOH. Analogously to bicelles made with the DMPE-DTPA/Ln^{3+} complex, the assemblies made with DMPE-Glu-DTPA/Ln^{3+} were sensitive to low pH values where the engineered Glu-DTPA head group of the phospholipid was protonated and no longer able to chelate Ln^{3+}.

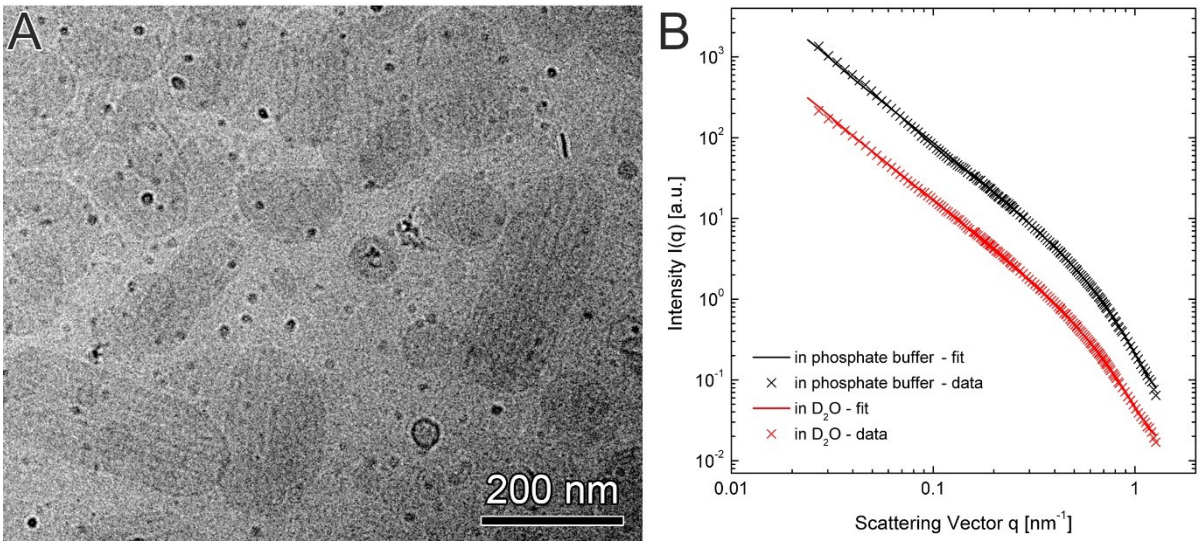

Figure S4. A) Cryo-TEM micrographs of DMPC/DMPE-Glu-DTPA/Tm^{3+} (molar ratio 4:1:1) in D_2O flash-frozen at 5 °C. The total lipid concentration was 15 mM. Ripples appear as regular darker lines on the planar surface of the polymolecular assemblies. The scale bar represents 200 nm. High contrast particles are ice crystals resulting from the freezing procedure. B) Radially averaged SANS curves (data points) and corresponding fits (filled lines) at 5 °C of DMPC/DMPE-Glu-DTPA/Tm^{3+} (molar ratio 4:1:1) produced in 50 mM phosphate buffer (black) and in D_2O (red). All samples were fitted with a form factor for Porod cylinders with a lognormal distribution. The disk thickness was 4.2 nm with an average radius and standard deviation of 94 nm and σ 0.23 for the sample in phosphate buffer and 95 nm and σ 0.27 for the sample in D_2O. The curves were shifted vertically for clarity.

Similar asymmetric assemblies were obtained for the of DMPC/DMPE-Glu-DTPA/Tm^{3+} (molar ratio 4:1:1) sample produced in D_2O as evidenced by the cryo-TEM micrograph in Figure S4A. The existence of ripples was not jeopardized by the absence of phosphate buffer. The radially averaged SANS curves in Figure S4B confirmed that the structure of the assemblies was not majorly affected when working in D_2O. Polydisperse species with an average radius of 95 nm were obtained, analogously to the system produced in phosphate buffer. These findings were further confirmed by DLS measurements where a hydrodynamic radius of 99 nm was obtained. Although the structural integrity of the assemblies was maintained when working in D_2O, the magnetic alignability was reduced. The alignment direction remained inverse and a thermoreversible collapse into magnetically non-alignable vesicles occurred at the phase transition temperature of DMPC at 24 °C. The phosphate buffer plays an integral role in guarantying the high magnetic response of DMPC/DMPE-Glu-DTPA/Ln^{3+}.

4. Fabrication considerations

The DMPC/DMPE-Glu-DTPA/Ln^{3+} (molar ratio 4:1:1) samples underwent the same fabrication procedure involving hydration of the dry lipid film with 50 mM phosphate buffer at a pH value of 7.4 and 5 freeze-thaw cycles in liquid nitrogen. The resulting suspension was extruded 10 times through polycarbonate membranes with a pore diameter of 200 nm at 40 °C for Chol-OH free samples and 60 °C for samples containing Chol-OH. These protocols are directly inspired from those employed for the fabrication of DMPC/DMPE-DTPA/Ln^{3+} based bicelle systems.[2,7,8] The extrusion step is not usually performed in bicelle fabrication.[10] However, extrusion is commonly employed to tailor the diameter of vesicles.[11] By extruding above the phase transition temperature, the DMPC/DMPE-DTPA/Ln^{3+} systems form vesicles whose size may be tailored by the pore diameter. By exploiting the thermo-reversible nature of these systems, the bicelles are readily regenerated from the extruded vesicles by cooling below the phase transition temperature to 5 °C. The resulting bicelle dimensions are intrinsically defined by the vesicles from which they were created. This offers another possibility of tailoring the magnetic alignability of the bicelles by altering their size without changing the composing lipid concentration or molar ratio. The DMPC/DMPE-Glu-DTPA/Ln^{3+} systems showed an analogous behavior by thermo-reversibly forming vesicles above the phase transition temperature T_m of DMPC. Therefore, their assembly size may also be indirectly tailored by extruding the vesicle precursors as shown herein.

The polymolecular assemblies obtained after the freeze thawing cycles were characterized by cryo-TEM in Figure S5A and by computing the radially averaged SANS curve in Figure S5B for a sample of DMPC/DMPE-Glu-DTPA/Tm^{3+} (molar ratio 4:1:1) at 5 °C. The cryo-TEM micrograph revealed a multitude of polydisperse assembly structures including folded planar assemblies, vesicles and multilamellar vesicles. The sample was also composed of similar asymmetric planar assemblies with ripples observed after extrusion (results not shown). The chaotic nature of the sample was confirmed by the SANS measurements in Figure S5B. Although the scattering intensity decayed with q^{-2}, confirming the existence of polymolecular assemblies made from a phospholipid bilayer, the data could not be fitted by any reasonable single geometry. The magnetic alignability of the sample was considerably hindered by the presence of vesicles structures, evidenced by the weak alignment factor A_f of 0.15 obtained at 5 °C and 8 T. The extrusion process is necessary to guaranty the formation of the more alignable planar DMPC/DMPE-Glu-DTPA/Tm^{3+} (molar ratio 4:1:1) species.

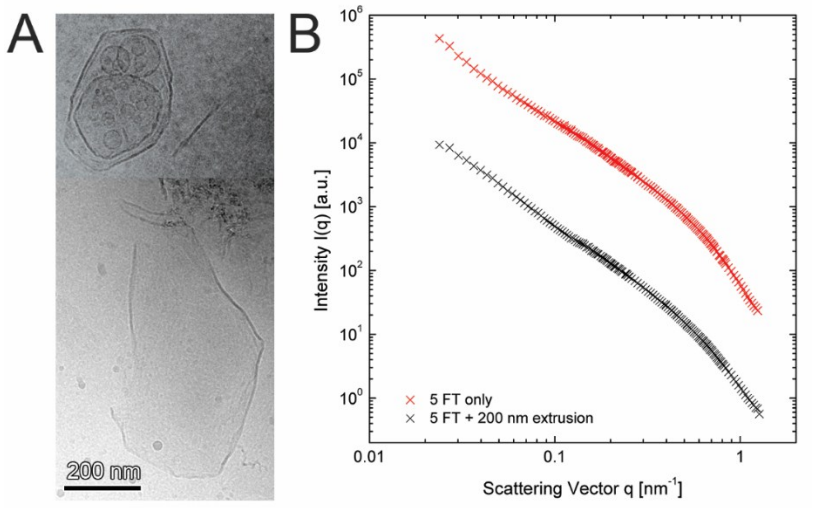

Figure S5. A) Cryo-TEM micrographs of DMPC/DMPE-Glu-DTPA/Tm^{3+} (molar ratio 4:1:1) after 5 freeze thawing (FT) cycles, flash-frozen at 5 °C. The total lipid concentration was 15 mM in a 50 mM phosphate buffer at a pH value of 7.4. A multitude of asymmetric structures are observed including vesicles and multilamellar vesicles (top) and large, partially folded assemblies (bottom). The scale bar represents 200 nm and is valid for both the top and bottom part of the composite image. High contrast particles are ice crystals resulting from the freezing procedure. B) Radially averaged SANS curves at 5 °C of DMPC/DMPE-Glu-DTPA/Tm^{3+} (molar ratio 4:1:1) after the 5 FT cycles (red) and after an additional 10 extrusions through a polycarbonate membrane with a pore diameter of 200 nm.

The sample was further extruded 10 times through a polycarbonate membrane with a pore diameter of 200 nm and another 10 times through a membrane with a pore diameter of 100 nm. The birefringence signal of the resulting sample was monitored on heating and cooling (1 °C/min) and compared to the reference extruded through 200 nm pores in Figure S6. The maximum birefringence signal obtained for the fully extruded sample was lower than that obtained for the reference sample extruded only through 200 nm pores. Since the birefringence signal is directly related to the magnetic alignment of the polymolecular assemblies, the lower magnetic alignment of the fully extruded sample likely originates from a smaller assembly size. Smaller assemblies have less lipids contributing to the cumulative magnetic energy of the assembly. The smaller size originates from the smaller precursor vesicles obtained by further extrusion through 100 nm pores. Analogously to DMPC/DMPE-DTPA/Ln^{3+} systems, extrusions may be applied for tailoring the size and magnetic response of DMPC/DMPE-Glu-DTPA/Ln^{3+} assemblies.

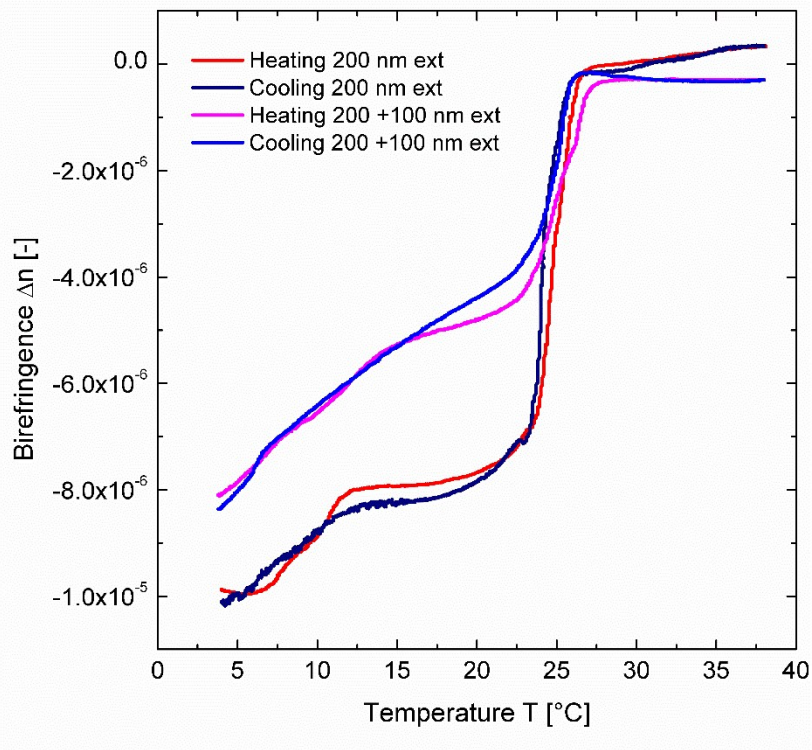

Figure S6. Evolution of the birefringence signal under a 5.5 T magnetic field as a function of temperature on heating and cooling (1 °C/min) for DMPC/DMPE-Glu-DTPA/Tm^{3+} (molar ratio 4:1:1) after 10 extrusions through a polycarbonate membrane with a pore diameter of 200 nm (red and dark blue) and another 10 extrusions through a membrane with a pore diameter of 100 nm (magenta and blue). The total lipid concentration was 15 mM in a 50 mM phosphate buffer at a pH value of 7.4.

5. Radially averaged SANS curves and fittings of DMPC/Chol-OH/DMPE-Glu-DTPA/Tm^{3+} (molar ratio 16:4:5:5)

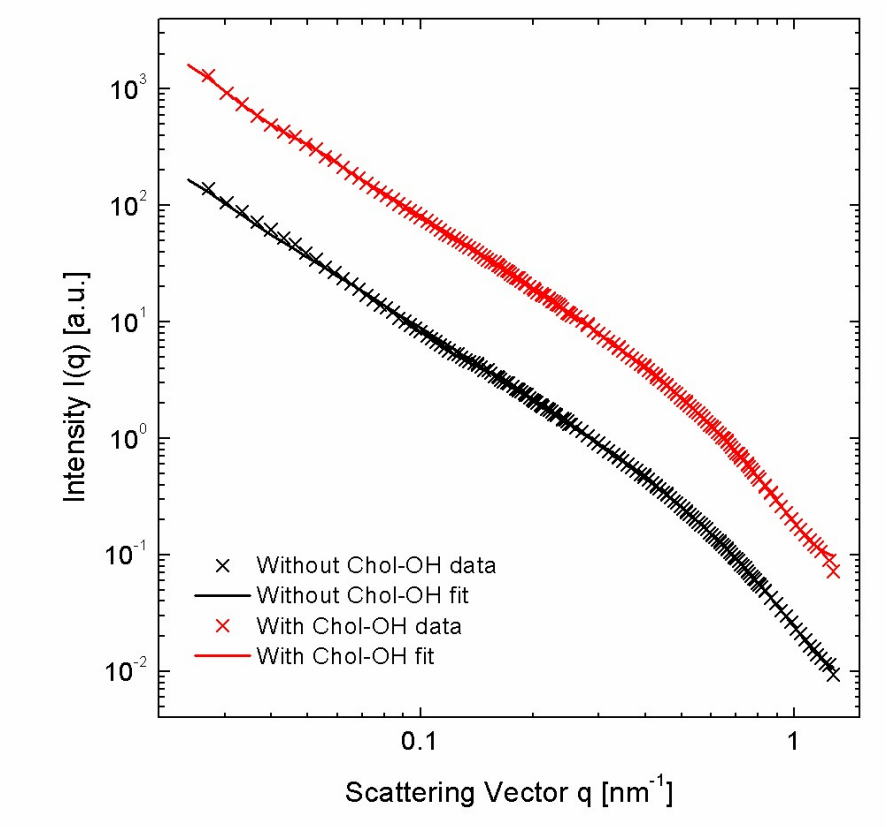

Figure S7. Radially averaged SANS curves and corresponding fit of DMPC/DMPE-Glu-DTPA/Tm^{3+} (molar ratio 4:1:1) and DMPC/Chol-OH/DMPE-Glu-DTPA/Tm^{3+} (molar ratio 16:4:5:5) at 5 °C. The total lipid concentration was 15 mM in a 50 mM phosphate buffer at a pH value of 7.4. The data for the Chol-OH doped assemblies was fitted with a form factor for Porod cylinders and a log normal distribution. The average radius was 104 nm, the bilayer thickness was 4.6 nm, and the standard deviation was 0.11. The curves were shifted vertically for clarity.

6. References

1. Micklitsch, C. M.; Yu, Q.; Schneider, J. P. Unnatural Multidentate Metal Ligating α-Amino Acids. *Tetrahedron Lett.* **2006**, *47*, 6277–6280.
2. Liebi, M.; Kuster, S.; Kohlbrecher, J.; Ishikawa, T.; Fischer, P.; Walde, P.; Windhab, E. J. Cholesterol-Diethylenetriaminepentaacetate Complexed with Thulium Ions Integrated into Bicelles to Increase Their Magnetic Alignability. *J. Phys. Chem. B* **2013**, *117*, 14743–14748.
3. Anelli, P. L.; Fedeli, F.; Gazzotti, O.; Lattuada, L.; Lux, G.; Rebasti, F. L-Glutamic Acid and L-Lysine as Useful Building Blocks for the Preparation of Bifunctional DTPA-like Ligands. *Bioconjug. Chem.* **1999**, 10, 137–140.
4. Gianella, A.; Mieszawska, A. J.; Hoeben, F. J. M.; Janssen, H. M.; Jarzyna, P. a; Cormode, D. P.; Costa, K. D.; Rao, S.; Farokhzad, O. C.; Langer, R.; et al. Synthesis and in Vitro Evaluation of a Multifunctional and Surface-Switchable Nanoemulsion Platform. *Chem. Commun.* **2013**, *49*, 9392–9394.
5. Yamada, S.; Kasai, Y.; Shioiri T. Diethylphosphoryl cyanide. A new reagent for the synthesis of amides. *Tetrahedron Lett*. **1973**, 18, 1595–1598.
6. (a) Son, W. S.; Park, S. H.; Nothnagel, H. J.; Lu, G. J.; Wang, Y.; Zhang, H.; Cook, G. A.; Howell, S. C.; Opella, S. J. "Q-Titration" of Long-Chain and Short-Chain Lipids Differentiates between Structured and Mobile Residues of Membrane Proteins Studied in Bicelles by Solution NMR Spectroscopy. *J. Magn. Reson.* **2012**, 214, 111–118. (b) De Angelis, A. a; Opella, S. J. Bicelle Samples for Solid-State NMR of Membrane Proteins. *Nat. Protoc.* **2007**, 2, 2332–2338.
7. Liebi, M. *Tailored phospholipid bicelles to generate magnetically switchable material.* PhD Thesis n° 21048, ETH Zürich, Switzerland, **2013**.
8. Liebi, M.; Kohlbrecher, J.; Ishikawa, T.; Fischer, P.; Walde, P.; Windhab, E. J. Cholesterol Increases the Magnetic Aligning of Bicellar Disks from an Aqueous Mixture of DMPC and DMPE-DTPA with Complexed Thulium Ions. *Langmuir* **2012**, 28, 10905–10915.
9. (a) Van Dam, L.; Karlsson, G.; Edwards, K. Direct Observation and Characterization of DMPC/DHPC Aggregates under Conditions Relevant for Biological Solution NMR. *Biochim. Biophys. Acta - Biomembr.* **2004**, *1664*, 241–256. (b) Mou, J.; Yang, J.; Shao, Z. Tris(hydroxymethyl)aminomethane ($C_4H_{11}NO_3$) Induced a Ripple Phase in Supported Unilamellar Phospholipid Bilayers. *Biochemistry* **1994**, *33*, 4439–4443. (c) Czajkowsky, D. M.; Huang, C.; Shao, Z. Ripple Phase in Asymmetric Unilamellar Bilayers with Saturated and Unsaturated Phospholipids. *Biochemistry* **1995**, *34*, 12501–12505.
10. (a) De Angelis, A.; Opella, S. J. Bicelle samples for solid-state NMR of membrane proteins. *Nat. Protoc.* **2007**, *2*, 2332–2338. (b) Avanti Polar Lipids Inc., *Bicelle Preparation*, https://avantilipids.com/tech-support/liposome-preparation/bicelle-preparation/, accessed: March 2017.
11. (a) Walde, P.; Cosentino, K.; Engel, H.; Stano, P.; Giant vesicles: preparations and applications. *ChemBioChem* **2010**, *11*, 848–865. (b) Avanti Polar Lipids Inc., *Liposome Preparation*, https://avantilipids.com/tech-support/liposome-preparation/, accessed: March 2017. (c) Avanti Polar Lipids Inc., *Preparing Large, Unilamellar Vesicles by Extrusion (LUVET)*, https://avantilipids.com/tech-support/liposome-preparation/luvet/, accessed: March 2017.